Jour. Korean Inst. Mining Geol.
Vol. 21, No. 2, P. 149−164 1988

Stable Isotope and Fluid Inclusion Studies of Gold-Silver--Bearing Hydrothermal-Vein Deposits, Cheonan-Cheongyang--Nonsan Mining District, Republic of Korea: Cheongyang Area

Chil-Sup So*, Shelton, K. L.**, Se-Jung Chi*, Sang-Hoon Choi*

Abstract: Electrum-sulfide mineralization of the Samgwang and Sobo mines of the Cheongyang Au-Ag area was deposited in two stages of quartz and calcite veins that fill fault zones in granite gneiss. Radiometric dating indicates that mineralization is Early Cretaceous age (127 Ma). Fluid inclusion and sulfur isotope data show that ore mineralization was deposited at temperatures between 340°and 180°C from fluids with salinities of 1 to 8 wt. % equiv. NaCl and a $\delta^{34}S_{\Sigma S}$ value of 2 to 5 per mil. Evidence of fluid boiling (and CO_2 effervescence) indicates a range of pressures from $<$ 200 to $\approx$ 700 bars, corresponding to depths of $\approx$ 1.5 $\pm$ 0.3 km in a hydrothermal system which alternated from lithostatic toward hydrostatic conditions. Au-Ag deposition was likely a result of boiling coupled with cooling.

Meaured and calculated hydrogen and oxygen isotope values of ore-forming fluids indicate a significant meteoric water component, approaching unexchanged paleometeoric water values. Comparison of these values with those of other Korean Au-Ag deposits reveals a relationship among depth, Au/Ag ratio and degree of water-rock interaction. All investigated Korean Jurassic and Cretaceous gold-silver-bearing deposits have fluids which are dominantly evolved meteoric waters, but only deeper systems ($\geq$ 1.5 km) are exclusively gold-rich.

INTRODUCTION

Most gold-silver vein deposits in Korea are intimately associated with major periods of Jurassic and Cretaceous granitic vulcanism (Shimazaki et al., 1981, 1986; So and Shelton, 1987 a, b; So et al., 1987a, b). Cretaceous granites have been shown to be higher level intrusions than Jurassic granites (Tsusue et al., 1981), providing an opportunity to investigate the influence of depth of emplacement on the postmagmatic evolution of granite-related gold systems.

Three types of deposits have been previously documented which display a consistent relationship among depth, water-to-rock ratio (degree of meteoric water involvement) and Au/Ag ratio (Shelton et al., 1988): Korean-type gold--silver deposits (Tsuchida, 1944); more silver-rich, epithermal deposits; and mesothermal gold-rich deposits (Shelton et al., 1988).

Korean-type deposits are most common, which are genetically associated with Late Jurassic-Early Cretaceous granites, and are characterized by high Au/Ag ratios (1:3 to 2:1) and a general paucity of sulfide minerals (Shikazono and Shimizu, 1986; Sugaki et al., 1986). Geochemical studies of Korean-type gold deposits indicate that gold deposition occurred at temperatures near 270°C in response to boiling and cooling at depths near 1.25 km (So and

* Department of Geology, Korea University, Seoul 132, Republic of Korea
** Department of Geology, University of Missouri, Columbia, Missouri 65211

Shelton, 1987a; So et al., 1987a).

The more silver-rich, epithermal deposits are genetically associated with Late Cretaceous--Tertiary granites and are characterized by lower Au/Ag ratios (1 : 10 to 1 : 200) and more abundant, complex sulfide mineralization. Geochemical studies of these deposits indicate that gold-silver deposition occurred at temperatures of < 240°C in response to boiling at depths of < 0.75 km (Park, 1983; So and Shelton, 1987b; So et al., 1987b).

Gold-rich, mesothermal deposits are associated with Jurassic (Daebo) vulcanism and are characterized by high Au/Ag ratios (5 : 1 to 8 : 1). Geochemical studies of these deposits indicate that gold deposition occurred at temperatures of 300° to 370°C in response to unmixing of CO_2-rich fluids at depths of > 4.5 km (Shelton et al., 1988).

Stable isotope and fluid inclusion studies of the Cheongyang area were undertaken because it contains a number of fissure-filling hydrothermal quartz veins cutting gneiss which contain gold, silver, copper, lead and zinc minerals. The Samgwang and Sobo mines are each located on such veins. Average gold grades range from 7 to 11 g/ton, with average Au/Ag ore ratios near 1 : 1.8.

In this paper we determine the age and nature of ore mineralization in the Cheongyang area, document the physical and chemical conditions of ore deposition, and compare the area's stable isotope systematics to those of other Au-Ag deposits in the Korean Peninsula.

GEOLOGY

The Cheongyang Au-Ag area is located approximately 125 km south-southeast of Seoul within the Precambrian Gyeonggi metamorphic belt of the Korean Peninsula (Fig. 1). The area is underlain by the Precambrian Gyeonggi gneiss complex. Two main rock units which unconformably overlie the precambrian gneisses are recognized in the mine area: the Early to Middle Jurassic Nampo Group of the Daedong Supergroup and the age unknown Yoogoo granite gneiss (Fig. 2). The Daedong Supergroup consists of the Bansong, Nampo and Kimpo Groups. The sedimentary strata of each of these Groups accumulated in isolated basins and their precise correlation, from basin to basin, has not been determined (Reedman and Um, 1975). All three Groups are bounded by major unconformities and all were folded and faulted during the Jurassic Daebo Orogeny.

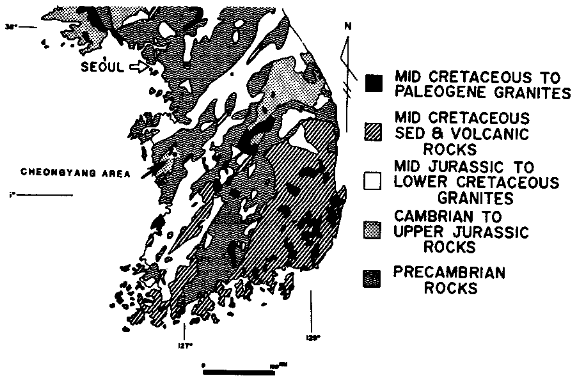

Fig. 1. General geologic map of the Republic of Korea showing the location of the Cheongyang Au-Ag area.

The mine area consists mainly of the Paegunsa Formation of the Upper Nampo Group which occurs as a massive xenolith in the Yoogoo granite gneiss and strikes N10° to 30°E and dips 35° to 80°NW or SE. The Paegunsa Formation consists of, in ascending stratigraphic order: conglomeratic sandstone with well-rounded chert pebbles; black shale; dark gray coarse sandstone; coaly shale; black shale; gray medium-grained sandstone; and fine-grained sandstone. Several thin coal seams are intercalated with black shales of the formation. Sandstones frequently contain thin calcareous beds.

The Yoogoo granite gneiss covers most of the mine area (Fig. 2) and frequently displays layered structuring of biotite-rich mafic mineral and felsic mineral bands. The Yoogoo granite gneiss is thought to have intruded the Paegunsa Formation during the Late Jurassic.

North-south-trending dikes consisting of melanoandesite and andesite porphyry (containing > 50% andesine plagioclase) have intruded all of the previously described rocks.

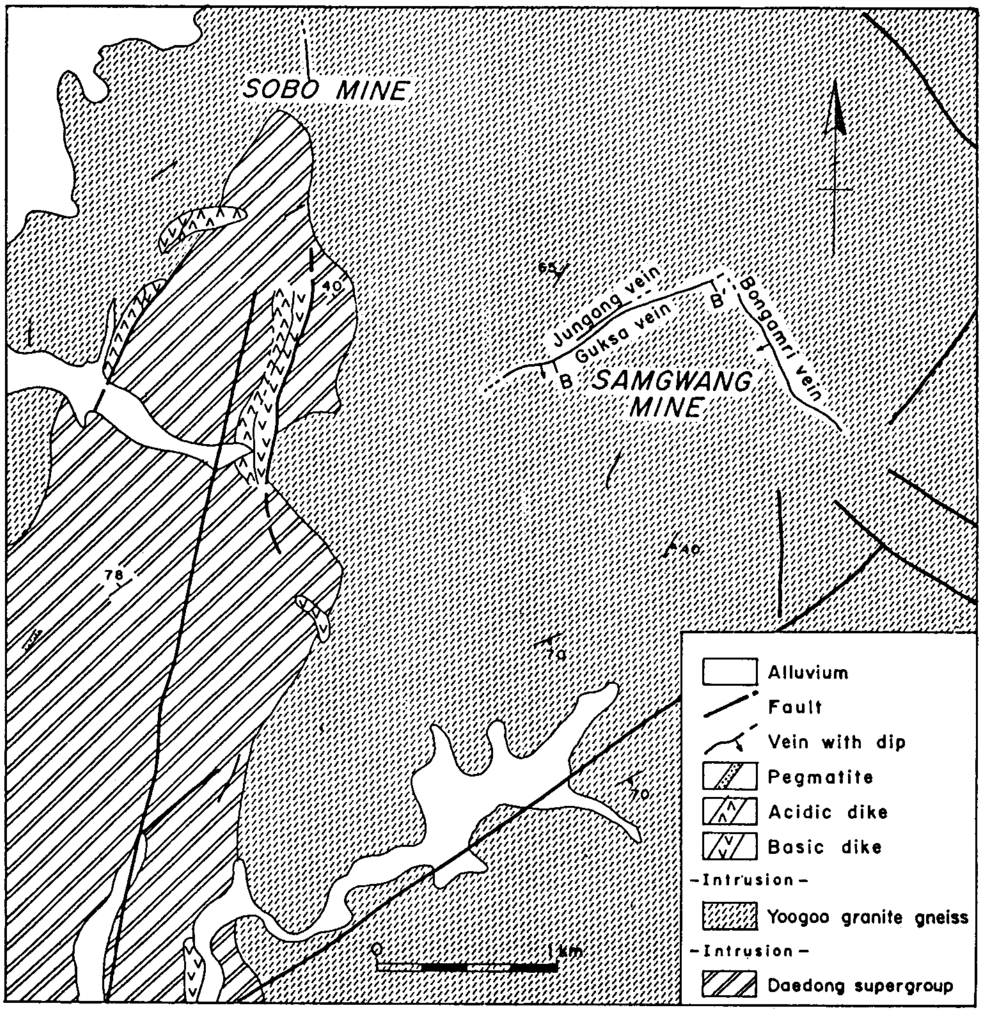

Fig. 2. Geologic map of the Cheongyang Au-Ag area.

VEINS

Within the Cheongyang mineralized area are a number of subparallel gold-silver-bearing hydrothermal quartz veins which were formed by narrow open-space filling of NE- and NW-trending fissures along structural planes in granite gneiss. The Samgwang and Sobo mines are deposited along such veins (Fig. 2). The Samgwang mine is comprised of the main productive Guksa vein with its parallel subsidiary Jungang vein, the Bongkamri vein with one small subsidiary vein and a barren calcite vein. Underground in the Samgwang mine, a pegmatite vein occurs which shows no direct genetic relationship to the gold vein.

The Guksa vein of the Samgwang mine is developed along a fault shear zone varying from 0.5 to 15 m in width. The zone has a trend of N50 — 60°E, an inclination of 35 — 70° SE and a total run of approximately 1.5 km. The vein pinches and swells repeatedly along strike and dip directions and ranges in thickness from 0.1 to 3.0 m, generally decreasing where the vein dip steepens. The Guksa vein shows en echelon structure where the thickness of the shear zone increases. The Jungang vein is less than 0.5 m thick and contains a smaller concentration of sulfide minerals (mostly arsenopyrite) than other mineralized quartz veins.

The Bongamri vein occurs along a N40 – 60°W-trending fault plane and varies in thickness from 0.1 to 0.8 m. The relationship between mineralization in the Guksa and Bongamri veins is enigmatic. In many places the veins are displaced by later fault movements and crosscut older acidic and intermediate dikes. The veins are themselves cut by younger dikes.

The main vein of the Sobo mine extends several hundred meters along a N10°W strike and is generally < 1.0 m in thickness.

Hydrothermal quartz veins of the Cheongyang area are mineralogically similar and consist mainly of milky quartz and sulfide minerals associated with gold. In the Samgwang mine two main irregularly tabular orebodies are recognized and are currently in production. The orebodies are normally < 400 m long and extend from the surface down to about 10 m above sea level, a vertical distance of 100 to 200 m. the orebodies contain relatively large concentrations of arsenopyrite, sphalerite, galena, chalcopyrite and pyrite. Electrum is intimately associated with compact aggregates of arsenopyrite and galena. The two orebodies are similar in ore controls and mineralogy. Generally the hanging-wall sides of the bodies are characterized by higher-grade sulfide mineral concentrations than the foot-wall sides. Though sulfide mineral aggregates are poorly disseminated throughout the veins, orebodies frequently display monomineralic arsenopyrite bands near vein margins. At some localities, milky quartz veinlets cementing wall-rock breccias display comb structures and contain minor galena, sphalerite and chalcopyrite.

Sulfide minerals associated with electrum vary inward from vein margins in the order: arsenopyrite + pyrite; galena + rare chalcopyrite; sphalerite + galena + chalcopyrite; galena + chalcopyrite; galena ± arsenopyrite. Orebodies are zoned compositionally with galena + sphalerite concentrated mostly in upper portions and arsenopyrite concentrated slightly at depth, though the veins contain a high concentration of arsenopyrite throughout (Fig 3.).

The Guksa vein of the Samgwang mine divides upward into two veins in the eastern

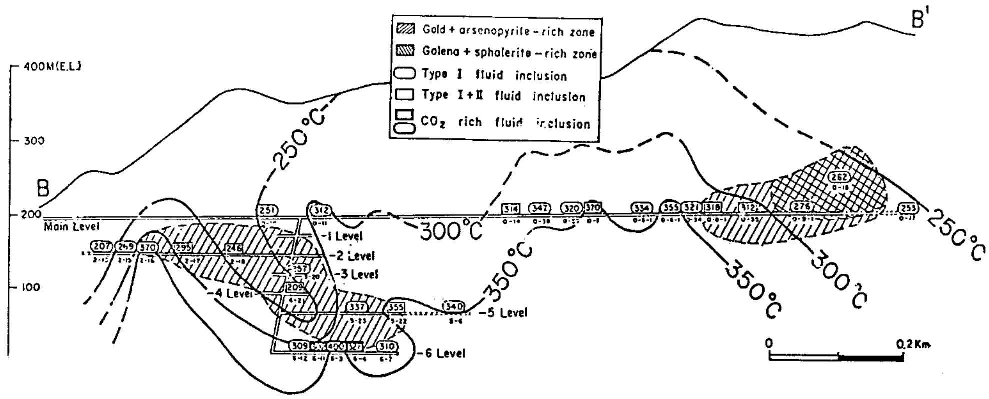

Fig. 3. Longitudinal cross-section B to B′ from Figure 2 projected onto the plane of the Guksa vein of the Samgwang mine demonstrating temperature variations associated with gold mineralization. Contoured isotherms show maximum homogenization temperatures of primary fluid inclusions in stage I minerals.

portion of level 1 of the vein. Here the vein thickness increases to 3 m and sulfides occur as masses on the foot-wall side. The Bongamri vein contains a smaller concentration of sulfides (mainly arsenopyrite) than the main vein.

Ore fluids have formed similar alteration haloes < 1 m from vein margins in wall rock of the two mines. Potassic (K-feldspathization) and argillic alteration (with addition of pyrite during wall-rock sulfidation) are more extensively developed than sericitic alteration in the host granite gneiss. Argillic alteration (mineralogy) is commonly foliated parallel to the main vein in the Samgwang mine. Rarely, conversion of orthoclase to albite occurs adjacent to gold-bearing quartz veins. Dikes intruded close to vein contacts have converted the intervening wall rock to dense hornfels containing disseminated pyrite.

DATING OF IGNEOUS ACTIVITY AND MINERALIZATION

Dates were obtained for the major igneous rock types and mineralized veins in the Cheongyang area using Rb-Sr and K-Ar methods (Table 1). The largest intrusion in the mining area, a biotite granite stock 20 km southeast of

Table 1. Rb—Sr and K—Ar Data of Specimens from the Cheongyang Au—Ag Area, Republic of Korea

A. Rb—Sr Data—Two—Point Isochron

Description	^{86}Sr (ppm)	^{87}Rb (ppm)	$^{87}Sr/^{86}Sr$	$^{87}Rb/^{86}Sr$	Isochron Parameters: Slope ($\times 10^{-3}$)	Isochron Parameters: Intercept	Isochron Parameters: Date (m. a. $\pm$ 1 σ)
Biotite granite							
Whole rock	45.9	39.3	0.7142	0.85	1.746(58)	0.7127 (8)	122.8±4.1
Biotite	9.70	151.1	0.7396	15.4			

B. K—Ar Data

Description	K (%)	Radiogenic ^{40}Ar (cc/g) STP $\times 10^{-6}$	Atmospheric ^{40}Ar (%)	Date (m. a. $\pm$ 1 σ)
Samgwang alteration sericite	4.88	24.98	8.2	127.1±2.8
Pegmatite underground in Samgwang mine K—feldspar	12.89	54.99	6.5	106.5±2.8
Pegmatite in mine area K—feldspar	8.09	21.91	4.4	68.4±1.7

the mines yielded a date of 122.8 ± 4.1 Ma using an Rb-Sr two-point isochron for biotite, indicating an Early Cretaceous age of emplacement. Potassium feldspar from pegmatitic veins, one underground in the Samgwang mine and the other near the mine area, yielded K-Ar dates of 106.5 ± 2.8 Ma and 68.4 ± 1.7 Ma respectively (Early and Late Cretaceous ages).

Sericite from a vein alteration halo in the Samgwang mine yielded a K-Ar date of 127.1 ± 2.8 Ma, indicating an Early Cretaceous age for gold-silver mineralization, likely associated with igneous activity similar to that of the biotite granite 20km to the southeast (122.8 ± 4.1 Ma). An Early Cretaceous age for mineralization in the Cheongyang area is in agreement with the observed mineralogy and gold/silver ratios of its deposits. Previous geochemical studies of other Au-Ag deposits in Korea (Shelton et al., 1988; So and Shelton, 1987a, b; So et al., 1987a, b) have shown that deposits with more complex parageneses including silver sulfides tend to be Cretaceous in age.

MINERALOGY AND PARAGENESIS

Vein mineralogy of all the orebodies is characterized by a monoascendant nature. The veins have similar mineral parageneses, though they contain variable gold concentrations, and have been divided into main paragenetic stages on the basis of textural and mineralogical relations of the veins: stage I, a quartz-sulfide-gold stage; stage II, a barren calcite stage (Fig. 4). The two stages are separated in time by tectonic fracturing events.

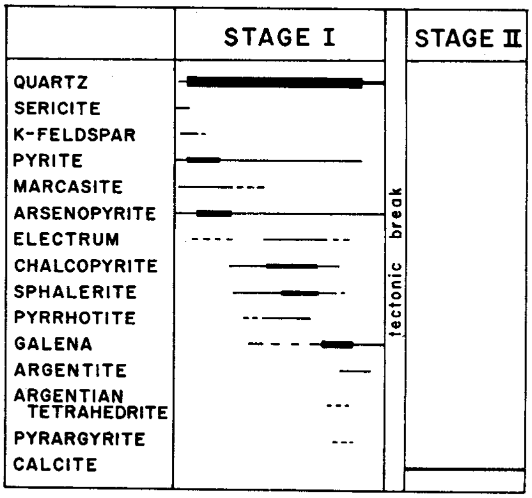

Fig. 4. Generalized paragenetic sequence of minerals from veins of the Cheongyang Au-Ag area. Width of lines corresponds to abundance.

Stage I

Economic quantities of gold, together with sulfides were introduced during this stage. Vein minerals consist mainly of milky, white and gray quartz, clear quartz in vugs, sericite, K-feldspar and various sulfides and electrum (Fig. 5). Veins of Stage I frequently display brecciated and poorly banded textures. The complete paragenetic sequence of minerals can be seen in distinct lateral mineral zonations within individual veins.

Fig. 5. Photograph of stage I milky quartz from the Guksa vein containing disseminated sulfides (Cp = chalcopyrite; Py = pyrite) and wall-rock breccia. Scale bar is 10 cm.

Quartz, the dominant mineral deposited during stage I, is massive in appearance. Frequently clear euhedral quartz crystals up to 1 cm are found in vugs that occur sporadically throughout the veins. Vugs also often contain sulfide minerals and strongly silicified wall-rock fragments containing potassium feldspar as an alteration product.

Pyrite (containing 23.7 ppm Co and 143 ppm Ni) occurs as a product of wall-rock sulfidation and as crystal aggregates or thin, massive bands within quartz matrix. These bands are intergrown with marcasite and rarely arsenopyrite, and are replaced by marcasite along grain margins.

Arsenopyite is the dominant sulfide mineral and occurs as fine to coarse disseminated grains and as monomineralic bands in intermediate to marginal portions of veins. Cataclastic arsenopyrite is found along vein margins in intimate assoiation with electrum. Within small vugs, arsenopyrite occurs with galena. Arsenopyrite is replaced and/or cemented along fractures and grain margins by galena, sphalerite and chalcopyrite.

Chalcopyrite is distributed rarely as coarse grains near vein margins and in intermediate portions of veins intergrown with sphalerite. Chalcopyrite is abundant only in orebodies of the main Guksa vein. Chalcopyrite frequently contains exsolved sphalerite and is replaced by galena.

Sphalerite (avg. 7.47 wt % Fe) occurs mainly in intermediate portions of veins. It is frequently intergrown with galena and chalcopyrite and is often replaced by galena along grain margins and cleavages. Where galena concentrations are greatest, sphalerite contains numerous chalcopyrite blebs.

The sphalerite-pyrite assemblage is considered to be a useful geothermometer for estimating formation temperatures of vein-type ore deposits. These minerals occur together within quartz veins of stage I in the Samgwang and Sobo mines. The mole fraction of FeS in sphalerite is ≈ 0.13. On the basis of the iron content of sphalerite and the presence of pyrite, the likely temperature and sulfur fugacity during this portion of stage I mineralization were (Barton and Skinner, 1979): $T \approx 340°C$; sulfur fugacity $\approx 10^{-9.8}$.

Pyrrhotite (containing 122 ppm Co and 87.1 ppm Ni) is limited to a few rare occurrences and is replaced by galena.

Galena occurs as interstitial fine grains throughout the veins and as massive aggregates in intermediate and vuggy portions. Galena+electrum veinlets fill fine fractures in arsenopyrite and pyrite. Galena infrequently crosscuts or replaces chalcopyrite and sphalerite (Fig. 6). Small grains of argentite occur in galena matrix.

Electrum (42.2 to 66.8 mole % Au) occurs as rounded grains and/or irregular wires with galena in fractures of fine-grained arsenopyrite and pyrite (Fig. 7). Infrequently electrum grains occur as inclusions in arsenopyrite.

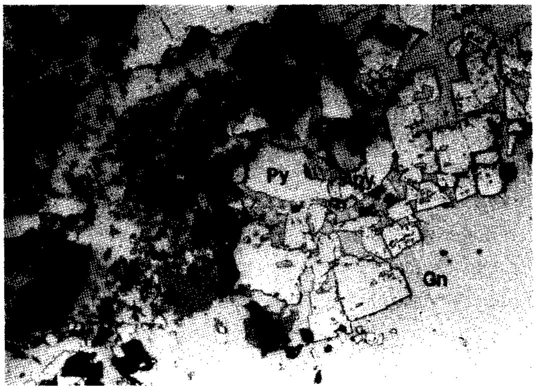

Fig. 6. Reflected light photomicrograph of stage I minerals in the Samgwang mine. Galena (Gn) replaces sphalerite (Sl) and subhedral to euhedral pyrite (Py) and arsenopyrite (Apy) along grain margins. Residual isolated sphalerite grains occur in a galena matrix. Scale bar is 0.1 mm.

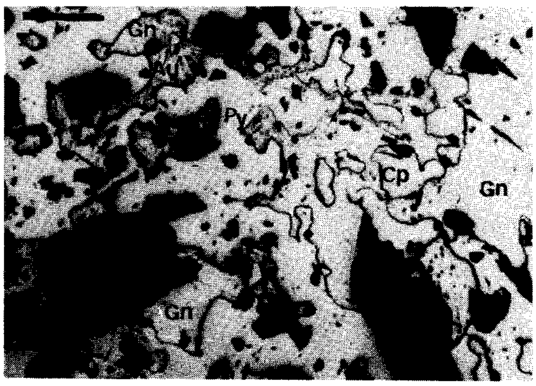

Fig. 7. Reflected light photomicrograph of stage I minerals from the Samgwang mine. Galena (Gn) associated with electrum (Au) replaces pyrite (Py) and chalcopyrite (Cp). Scale bar is 0.1mm.

Stage II

Stage I closed with an episode of fracturing which opened new space for the introduction of minor calcite veins of stage II. These barren, massive calcite veins disappear upward and contain rarely small vugs with clear, euhedral calcite rhombs.

FLUID INCLUSION STUDIES

Specimens from 94 localities were examined to investigate variations of fluid temperature and composition throughout the mining area (Fig. 3). Minerals examined were quartz, sphalerite and calcite. Some samples chosen were euhedral quartz crystals from vugs of the Samgwang mine, which allowed us to document fluid variations temporally. Most inclusions examined were < 40 μm in diameter.

Three types of fluid inclusions were observed at the Samgwang mine and are classified according to the terminology of Nash (1972):

Type I: This dominant type of inclusion found in all samples studied is liquid-rich and contains a liquid and a small bubble comprising 5 to 25 volume % of each inclusion. Type I inclusions vary in size from 4 to 30 μm in diameter and are generally ellipsoidal or equant in shape. Crushing indicates that small quantities of CO_2 are infrequently present in some type I inclusions in quartz and sphalerite.

Type II: Type II inclusions are vapor-rich and have bubbles comprising > 60 volume % of each inclusion. They occur as primary and secondary inclusions in quartz and sphalerite and range in size from 4 to 30 μm. Inclusion types I and II occur together in many quartz and sphalerite samples.

Type IV: These inclusions contain three phases: liquid water, liquid CO_2 and vapor

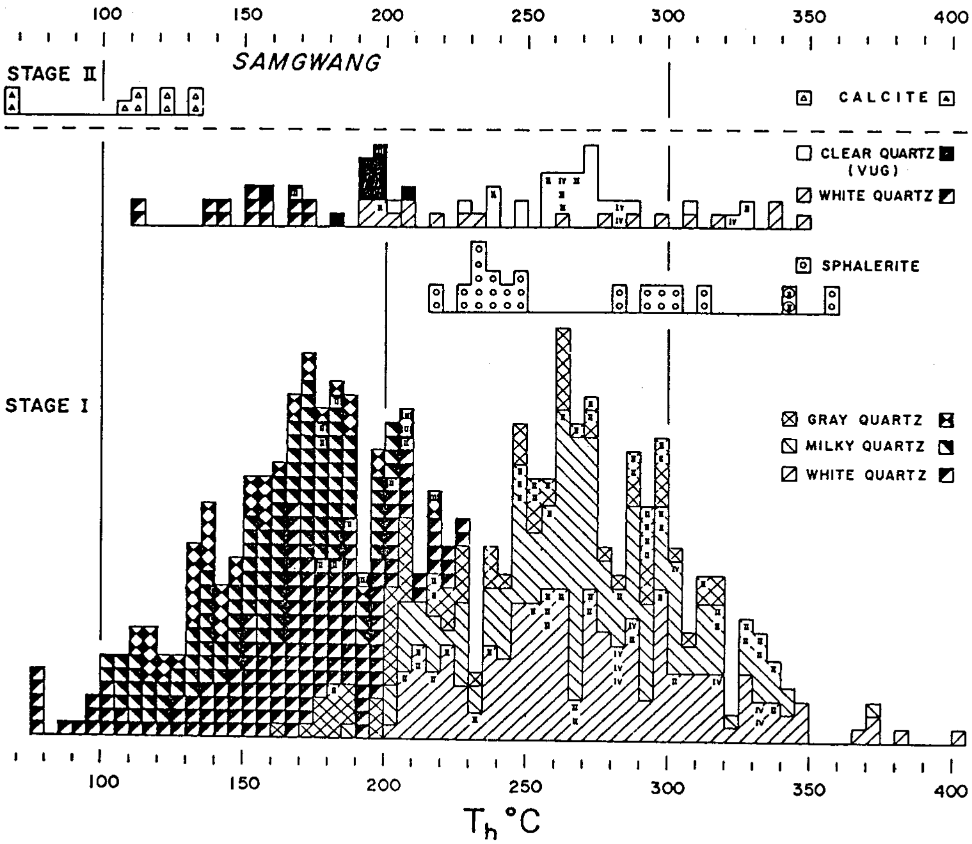

Fig. 8. Frequency diagram of homogenization temperatures of primary and secondary fluid indlusions in stage I and II vein minerals of the Samgwang mine(II =vapor-rich inclusions; IV= liguid-CO_2-bearing inclusions).

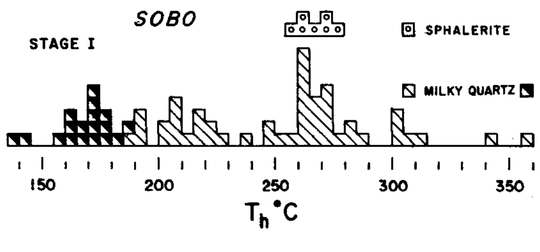

Fig. 9. Frequency diagram of homogenization temperatures of primary and secondary fluid inclusions in stage I vein minerals of the Sobo mine.

CO_2. The volume percentages of each phase at 17°C are: 42 to 62 %; 31 to 53%; and 5 to 10%, respectively. Type IV inclusions range from 10 to 40 μm in diameter and occur only as primary inclusions in quartz. They are frequently associated with inclusion types I and II.

Inclusions in Stage I

Quartz of stage I contains dominantly type I inclusions, frequently associated with inclusion types II and III. Primary inclusions of type II occur mainly in quartz specimens from ore shoots. Quartz veins from the Samgwang mine contain largest and most abundant type II inclusions. Sphalerite contains primary and secondary inclusions of type I and II.

CO_2-rich type IV inclusions (10 to 40 μm) are dominant in clear euhedral quartz from vugs in veins of the Samgwang mine. They occur as primary inclusions in other vein quartz only in deeper portions of the Samgwang mine and typically exhibit negative crystal morphologies. Calculated fluid compositions (mole %) of type IV inclusions (using the method of Kelly and Rye, 1979) are: H_2O (67.0 to 81.8%); CO_2 (13.9 to 28.1%); NaCl (4.2 to 4.9%).

Homogenization temperatures of primary inclusions in stage I minerals from the Samgwang and Sobo mines (Figs. 8 and 9) range from 164° to 400°C and 187° to 355°C, respectively. Homogenization temperatures of primary inclusions in the Guksa, Bongamri and Jungang veins of the Samgwang mine range from 164° to 400°C, 214° to 365°C, and 217° to 265°C, respectively.

Primary inclusions in the various types of quartz from the Samgwang mine have the following ranges: white quartz (type I, 192° to 400°C; type II, 197° to 338°C; type IV, 283° to 330°C); milky quartz (type I, 189° to 370°C; type II, 247° to 337°C; type IV, 302°C); gray quartz (type I, 164° to 318°C; type II, 183° to 314°C); and clear quartz (type I, 204° to 326°C; type II, 239° to 327°C; type IV, 264° to 324°C). Homogenization temperatures of primary inclusions of type I in milky quartz from the Sobo mine are 187° to 355°C. Note that type IV inclusions have consistently higher homogenization temperature ranges that those of type I and II inclusions.

Salinities of primary inclusions in quartz from the Samgwang mine range from 1.2 to 7.9 wt. % equiv. NaCl (Fig. 10). Salinities of fluids from quartz in the Guksa, Bongamri and Jungang veins of the Samwang mine range from 2.1 to 7.9, 1.2 to 6.3 and 5.0 to 6.6 wt. % equiv. NaCl, respectively. Salinities of inclu-

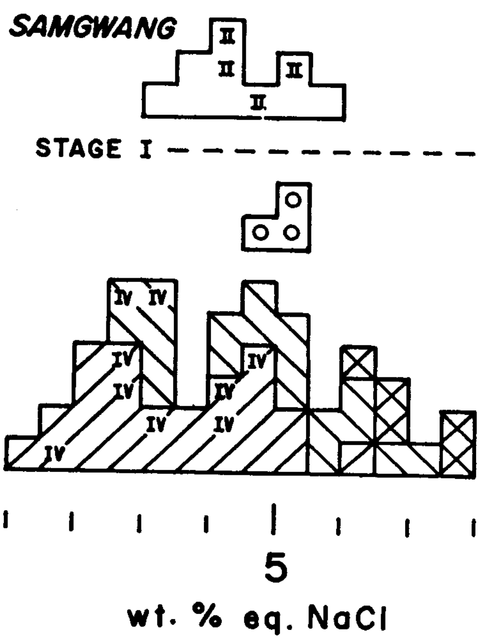

Fig. 10. Frequency diagram of salinities of fluid inclusions in vein minerals of the Samgwang mine. Symbols are the same as in Figures 8 and 9.

sions in various types of quartz from the Samgwang mine have the following ranges (wt. % equiv. NaCl): white quartz (type I, 1.2 to 6.3 ; type IV, 1.7 to 4.8); milky quartz (type I, 2.9 to 7.4; type IV, 2.9 to 3.4); gray quartz (type I, 6.1 to 7.9); clear quartz in vugs (type I, 3.1 to 5.8; type II, 4.2 to 5.2).

Primary inclusions in sphalerite have the following homogenization temperature ranges: Samgwang mine (type I, 218° to 355°C; type II, 340°C); Sobo mine (type I, 258° to 278°C). Salinities of primary inclusions of type I in sphalerite range from 4.6 to 5.4 wt. % equiv. NaCl.

Inclusions in Stage II

Primary and secondary inclusions of type I in stage II calcite from the Jungang vein of the Samgwang mine are small (mainly 8 to 15 μm). Primary inclusions homogenize from 106° to 130°C. Salinities were not determined due to the unsuitability of inclusions for freezing studies.

Relationship Between Homogenization Temperature and Salinity

The relationship between homogenization temperature and salinity in stage I veins of the Samgwag mine (Fig. 11) indicates a history of cooling and dilution following boiling (and/or CO_2-effervescence). Fluid boiling (unmixing) at initial high temperatures of ≈ 300° ± 25°C led to increase in salinity. Later cooling and dilution of ore-forming fluids by mixing with less-evolved, CO_2-poor, meteoric waters (See STABLE ISOTOPE STUDIES) resulted in the linear relationship between to temperature and salinity shown in Figure 11.

The presence of abundant type II and IV inclusions correspondes closely to gold ore shoots at reconstructed maximum temperature isotherms near 300° ± 25°C (Fig. 3). We therefore interpret gold deposition to be a result of cooling associated with fluid mixing and dilution of a boiling fluid.

Pressure Considerations and Significance of Boiling

Where liquid-rich type I and vapor-rich type

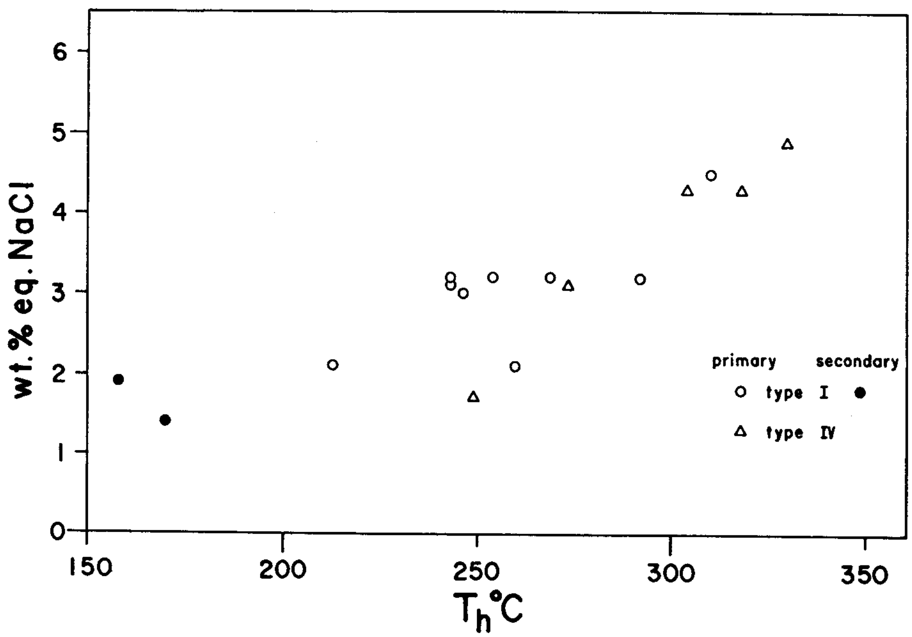

Fig. 11. Salinity vs. homogenization temperature diagram for primary secondary type I and IV inclusios from the Samgwang mine.

II inclusions occur together, they homogenize at nearly the same temperature, indicating that ore fluids boiled throughout the mineral paragenesis at temperatures of < 340°C to > 200°C (Fig. 8). Data for the system H_2O-NaCl (Sourirajan and Kennedy, 1962; Haas, 1971), combined with temperature and salinity data for these inclusions, indicate minimum pressures of < 200 to 300 bars.

When the presence of CO_2 in type IV inclusions is considered (See Inclusions in Stage I Veins), higher pressures are indicated for the early, higher-temperature portions of the paragenesis (324° to 264°C). Fluid unmixing in the system H_2O-CO_2-NaCl with a CO_2 content of ≈ 15 to 30 mole % and 4 wt. % NaCl indicates pressures of ≈ 500 to 700 bars (Bowers and Helgeson, 1983a, b).

Calculations for all data indicate formation pressures in the range of < 200 to ≈ 700 bars. This range of pressures corresponds to depths of boiling (and CO_2 effervescence) of ≈ 1.5 ± 0.3 km in a hydrothermal system which alternated from lithostatic toward hydrostatic conditions.

Boiling in hydrothermal systems can result in abrupt chemical changes (e.g. oxygen fugacity, ΣH_2S) in the liquid phase (Drummond, 1981; Drummond and Ohmoto, 1985) which may favor deposition of precious metals through destabilization of metal complexes, such as $Au(HS)_2^-$ and $AgCl_2^-$ (Seward, 1984; Cole and Drummond, 1986). We interpret gold deposition in the Cheongyang area to be a result of boiling coupled with cooling.

STABLE ISOTOPE STUDIES

Recent studies have demonstrated the usefulness of stable isotopes in elucidating the origin and history of hydrothermal fluids and their

Table 2. Sulfur Isotope Data for Mines of the Cheongyang Au–Ag Area, Republic of Korea

Mine	Sample No.	Mineral	$\delta^{34}S$ (‰)	$\Delta^{34}S$ (‰)	T℃
Cheongyang	0–6–1	galena	2.0	sp–gn	
(Guksa Vein)		sphalerite	4.0	2.9	329±37
		arsenopyrite	5.1		
	0–6–2	chalcopyrite	3.0		
		arsenopyrite	4.1		
	0–8	galena	0.6		
	0–9–1	chalcopyrite	3.7		
		sphalerite	3.5		
	2–16	galena	1.5		
		sphalerite	2.9		
	2–17	galena	1.8		
		arsenopyrite	5.1		
		chalcopyrite	4.1		
	4–21	arsenopyrite	5.0		
		galena	1.1	sp–gn	
		sphalerite	5.0	3.9	162±30
	5–22	arsenopyrite	5.2		
		sphalerite	5.0		
Sobo	1–1	pyrite	3.6	py–cp	
(Main vein)		chalcopyrite	1.9	1.7	234±56
	1–8	galena	0.7	sp–gn	
		sphalerite	3.2	2.5	262±34
	1–8–1	galena	0.6		
	1–11	arsenopyrite	4.0		

Table. 3. Carbon, Oxygen and Hydrogen Isotope Data for Calcite, Quartz and Their Inclusion Fluids, Samgwang Mine, Cheongyang Au−Ag Area, Repulic of Korea

Sample No.	Mineral	$\delta^{13}C$ (‰)	$\delta^{18}O$ (‰)	T℃[1]	$\delta^{18}O$water(‰)[2]	δD (‰)
0−8−1	gray quartz		7.6	300	+0.1	−90
0−18	gray quartz		7.9	250	−1.5	
2−17	white quartz		7.7	250	−1.7	−102
4−21	white quartz		5.7	210	−5.9	
6−3	white quartz		5.2	350	−0.6	
3−1	calcite	−4.0	9.4	130	−4.8	−129
3−21	calcite	−3.9	10.3	130	−3.9	−130

1. Based on fluid inclusion temperatures
2. Calculated water compositions based on quartz-water and calcite-water oxygen isotope fractionations of O'Neil et al. (1969) and Clayton et al. (1972), respectively

constituents in vein-type gold-silver deposits. In this study we measured the C, O, H and S isotope compositions of quartz, calcite, sulfides and fluid inclusion waters. Standard techniques for extraction and analysis were used (McCrea, 1950; Grinenko, 1962; Roedder et al., 1963; Hall and Friedman, 1963; Rye, 1966). Data are reported in standard δ notation relative to the PDB standard for C, SMOW for O and H, and CDT for S. The analytical error is approximately ± 0.1 per mil for C, O and S ; ± 2 per mil for H (Tables 2 and 3).

Sulfur Isotope Study

The $\delta^{34}S$ values (per mil) of 24 hand−picked sulfides from the Samgwang and Sobo mines have the following ranges (Table 2): arsenopyrite (4.0 to 5.2); chalcopyrite (1,9 to 4.1); sphalerite (2.9 to 5.0); galena (0.6 to 2.0); pyrite (3.6). Three sphalerite-galena pairs with textures suggesting coprecipitation of the phases have $\Delta^{34}S$ values of 3.9 to 2.0 per mil, yielding temperatures of 162° ± 30°C to 329° ± 37°C, respectively. A pyrite-chalcopyrite pair has a $\Delta^{34}S$ value of 1.7 per mil, yielding a temperatures of 234° ± 56°C. These calculated temperatures are in good agreement with homogenization tempereratures of primary fluid inclusions in associated quartz.

Using temperatures estimated from fluid inclusions, sulfur isotope pairs and paragenetic constraints, calculated $\delta^{34}S$ values of H_2S in hydrothermal fluids of stage I are 2.1 to 4.9 per mil (Ohmoto and Rye, 1979). The ore mineral assemblage pyrite + pyrrhotite and the alteration assemblage muscovite + quartz + K-feldspar indicate that sulfur in the hydrothermal fluids was dominantly H_2S. Therefore the $\delta^{34}S$ values of H_2S (2 to 5 per mil) are a good approximation of the $\delta^{34}S_{\Sigma S}$ value of the fluid. We interpret these values to represent an igneous source of sulfur, possibly the nearby biotite granite.

Oxygen and Carbon Isotope Study

The $\delta^{18}O$ values (per mil) of 5 quartz samples from the Samgwang mine are: white quartz, 5.2 to 7.7‰; gray quartz, 7.6 to 7.9‰ (Table 3). Calculated $\delta^{18}O$ water values (per mil), using the fractionation equation of Clayton et al. (1972), are: white quartz, -0.6 to -1.7‰; gray quartz, 0.1 to -1.5‰.

The $\delta^{18}O$ values of two stage II calcites from the Samgwang mine are 9.4 and 10.3 per mil. Their $\delta^{13}C$ values are -4.0 and -3.9 per mil, respectively. Calculated $\delta^{18}O$ water values, using the fractionation equation of ÓNeil et al. (1969), are -4.8 and -3.9 per mil (Table 3).

Hydrogen Isotope Study

Inclusion waters were extracted from 2 quartz and 2 calcite samples. Their δD values (per mil) are: white qurartz, -102‰; gray quartz, -90‰; calcite, -129 to -130‰(Table 3).

INTERPRETATION OF ISOTOPE RESULTS

In order to assess the importance of meteoric, magmatic and metamorphic waters in the Jungwon gold-mineralized mesothermal systems and interpret the measured δD values of inclusion waters, it is important to know the δD value of local meteoric water at the time of mineralization. The measured range of δD values for fluids from shallow (<1.25 km), Cretaceous (142 to 68 Ma) Au-Ag-bearing deposits in Korea is -81 to -143 per mil (So and Shelton, 1987a, b; So et al., 1987a, b; Shelton et al., 1988; Shelton and So, unpublished data) and is assumed to represent the range of paleometeoric water compositions near the time of mineralization. Such a wide range of hydrogen isotope compositions is not surprising, because modern surface waters in the Republic of Korea display large hydrogen isotope variations (Kim and Nakai, 1981, 1987): rain waters (+2 to -141 per mil); ground waters (-42 to -73 per mil); hot spring waters (-39 to -77 per mil).

Figure 12 shows the measured and calculated fluid compositions of the Cheongyang Au-Ag area (Samgwang mine) on a conventional hydrogen versus oxygen isotope diagram. The range of these data is consistent with meteoric water interaction as fluid compositions approach those of local unexchanged paleometeoric waters. Significant meteoric water involvement is not surprising in the relatively shallow (< 1.5 km) Au-Ag system.

For comparison, data from Cretaceous and Jurassic Korean gold-silver deposits are also shown in Figure 12 and Table 4. All of the data display various degrees of ^{18}O-enrichment relative to meteoric water, produced by exchange with hot igneous rocks, the classic ^{18}O-shift (Taylor, 1974). However, individual mines and districts have relatively narrow ranges of hydrogen and oxygen isotope compositions which are directly related to their gold/silver ratios and which reflect their depths of formation. Silver-rich epithermal deposits (Nonsan, Yangpyeong-Weonju, and Yeoju) dis-

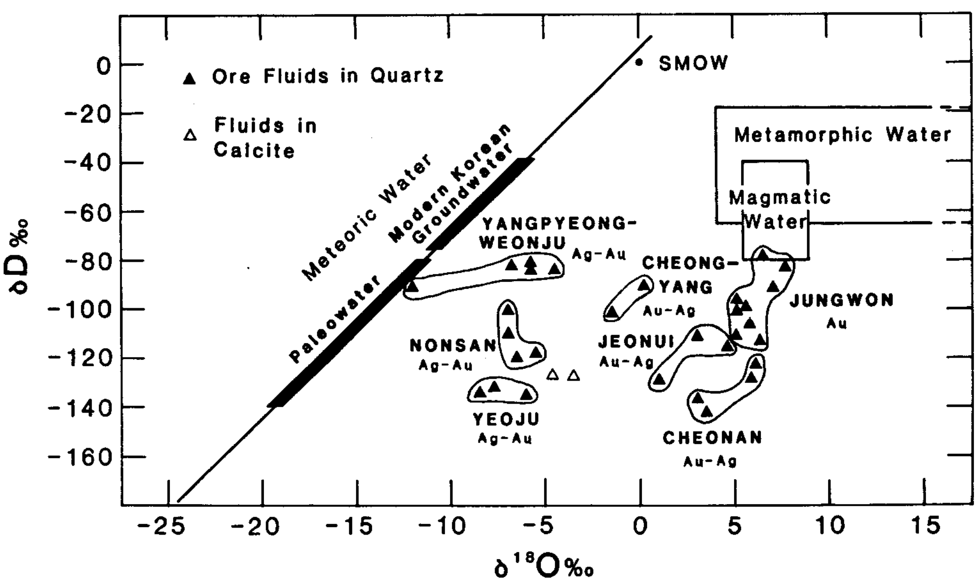

Fig. 12. Hydrogen vs. oxygn isotope diagram displaying stable isotope systematics of hydrothermal fluid compositions in Korean gold-silver depossits. All of the data are consistent with various degrees of $_{18}O$ and D enrichment relative to paleometeoric waters, which are directly related to gold/silver ratioss of the depossits(See INTRODUCTION).

Table 4. Characteristics of Au-Ag Vein Deposits of the Republic of Korea

	Epithermal	Korean-Type	Mesothermal
Age	Late Cretaceous - Tertiary	Early–Late Cretaceous	Jurassic
Depth of Formation	<750m	750 to 1,500m	>4.5 km
Petrology of Host Units	Granites, volcanic, sedimentary & meta morphic rocks	Granites, meta-morphic rocks	Granitic gneisses
Structural Setting			
Regional:	Calderas, volcanic centers	Volcanic centers, fault zones	Fault zones
Deposit Scale:	Faults & phreatic breccias	Faults and fault breccia zones	Faults parallel to foliation
Ores			
Mineralogy:	Complex, multiple stages, quartz & carbonate veins, sulfosalts, distinct base-& precious-metal zones, electrum = 55 – 70mole %Ag	Simple, multiple stages, quartz veins, argentite . electrum = 35 – 60 mole %Ag	Simple, single stage, massive quartz veins, rare sulfides native gold
Textures:	Stockwork, vein filling comb structures, crusts, veins <0.01–0.25m wide	Vein filling, banded structures, veins 0.1–1.2m wide	Massive veins, 0.1–1.0 m wide, ore shoots up to 200 m
Au / Ag Ratio:	1:10 – 1:200	1:3 – 2:1	5:1 – 8:1
Hydrothemal Alteration	Strong, silicification, advanced argillic, potassic, propylitic	Moderate, silici-fication, sericitic, argillic, propylitic	Weak, sericitic, propylitic, chloritic
Gold Depositing Fluids	<240℃, low CO_2	225°–300℃, low CO_2	300°–370℃ intermediate to high CO_2
Stable Isotope Data*	$\delta^{18}O$ = –13.1 to –4.2	$\delta^{18}O$ = –1.7 to 5.5	$\delta^{18}O$ = 5.0 to 7.7
Ore Deposition Mechanism(s)	Boiling, wall rock alteration, dilution	Boiling, cooling	Unmixing (CO_2 effervescence)

*Measured and calculated ore fluid values (per mil) relative to SMOW

References: Park (1983); Shelton et al. (1988); So and Shelton (1987a, b); So et al. (1987a, b); Sugaki et al. (1986)

play the smallest ^{18}O shifts, indicating a lesser degree of water-rock interaction (high water/rock ratios) at shallow depths of formation (< 750 m). Korean-type gold-silver deposits (Cheongyang, Jeonui, Cheonan) display ^{18}O shifts intermediate to those of epithermal and mesothermal deposits, indicating an intermediate degree of water-rock interaction at moderate depths of formation (750 to 1,250 m). Mesothermal gold deposits (Jungwon) display the largest ^{18}O shifts, indicating the highest degree of water-rock interaction (lowest water/rock ratios) at relatively great depths of formation (> 4.5 km).

This suggests a relationship between depth and degree of water-rock interaction in Korean deposits. All of these gold-silver-bearing deposits have fluids which are dominantly evolved meteoric waters, but only deeper systems with higher degrees of igneous rock interaction are exclusively gold-rich.

ACKNOWLEDGEMENTS

This research was supported by grants from the Korean Science and Engineering Foundation to C.S. So and the national Science Foundation's U.S.-Republic of Korea Cooperative Research Program (INT 85−17627) to K.L. Shelton. Stable isotope analyses were performed in the laboratories of D.M. Rye, Yale University.

REFERENCES

Barton, P.B., Jr., and Skinner, B.J. (1979) Sulfide mineral stabilities, in Barnes, H. L., ed., Geochemistry of hydrothermal ore deposits: New York, Wiley and Sons, p. 278-403.

Clayton, R.N., O'Neil, J.R., Mayeda, T. (1972) Oxygen isotope exchange between quartz and water: Jour. Geophys. Research v. 77, p. 3035-3067.

Cole, D. R., and Drummond, S. E. (1986) The effect of transport and boiling on Ag/Au ratios in hydrothermal solutions: A preliminary assessment and possible implications for the formation of epithermal precious-metal ore deposits: Jour. Geochem. Explor., v. 25, p. 45-79.

Drummond, S.E. (1981) Boiling and mixing of hydrothermal fluids: Chemical effects on mineral precipitation: Unpub. Ph.D. thesis, Pennsylvania State Univ., 380 p.

Drummond, S. E., and Ohmoto, H. (1985) Chemical evolution and mineral deposition in boiling hydrothermal systems: Econ. Geol., v. 80, p. 126-147.

Grinenko, V.A. (1962) Preparation of sulfur dioxide for isotopic analysis: Zeitschr. Neorgan. Khimii, v. 7, p. 2478-2483.

Haas, J.L., Jr. (1971) The effect of salinity on the maximum thermal gradient of a hydrothermal system at hydrostatic pressure: Econ. Geol., v. 66, p. 940-946.

Hall, W.E., Fried man, I. (1963) Compositions of fluid inclusions, Cave-in-Rock fluorite district, Illinois, and Upper Mississippi Valley zinc-lead district: Econ. Geol., v. 58, p. 886-911.

Kelly, W.C., and Rye, R.O. (1979) Geologic, fluid inclusion, and stable isotope studies of the tin-tungsten deposits of Panasqueira, Portugal: Econ. Geol., v. 74, p. 1721-1822.

McCrea, J.M. (1950) The isotope chemistry of carbonates and a paleotemperature scale: Jour. Chem. Phys., v. 18, p. 849-857.

Nash, J.T. (1972) Fluid inclusion studies of some gold deposits in Nevada: U.S. Geol. Surv. Prof. Paper 800-C, p. 15-19.

Ohmoto, H., and Rye, R.O. (1979) Isotopes of sulfur and carbon. In Barnes, H.L., ed, Geochemistry of Hydrothermal ore Deposits, 2nd Ed., New York: Wiley and Sons, p. 509-567.

O'Neil, J.R, Clayton, R.N., Mayeda, T.K. (1969) Oxygen isotope fractionation in divalent metal carbonates: Jour. Chem. Phys., v. 51, p. 5547-5558.

Park, H. I. (1983) Ore and fluid inclusions of the Tongyeong gold-silver deposits: Jour. Korean Inst. Mining Geology, v. 16, p. 245-251 (in Korean).

Roedder, Ingram, B., Hall, W.E. (1963) Studies or fluid inclusions. III. Extraction and quantitative analysis of inclusions in the milligram range: Econ. Geol., v. 58, p. 353-374.

Rye, R.O. (1966) The carbon, hydrogen, and oxygen isotopic compositions of hydrothermal fluids responsible for the lead-zinc deposits at providencia, Zacatecas, Mexico: Econ. Geol., 61, p. 1339-1427.

Seward, T,M. (1984) The transport and deposition of gold in hydrothermal systems, in Foster, R.P., ed., Gold '82: The Geology, Geochemistry and genesis of Gold Deposits, Geol. Soc. Zimbabwe Spec. Pub. 1, p. 165-181.

Shikazono, N., and Shimizu, M. (1986) Compositional variations in Au-Ag series mineral from some gold deposits in the Korean peninsula: Mining Geology, v. 36, p. 545-553.

Shimazaki, H., Sato, K., and Chon, H. T. (1981) Mineralization associated with Mesozoic felsic magmatism in Japan and Korea: Mining Geology, v. 31, p 297-310.

Shimazaki, H., Lee, M.S., Tsusue, A., and Kaneda, H. (1986) Three epochs of gold mineralization in South Korea: Mining Geology, v. 36, p. 265-272.

Shelton, K.L., So, C.S., and Chang, J.S. (1988) Gold-rich mesothermal vein deposits of the Republic of Korea: Geochemical studies of the Jungwon gold area: Econ. Geol. (in press).

So, C.S., Chi, S.J., and Shelton, K.L. (1987a) Stable isotope and fluid inclusion studies of gold-silver-bearing vein deposits, Cheonan-Nonsan mining district, Republic of Korea: 3 Nonsan area: Neues Jahrb. Mineral. Abhand., v. 158, p. 47-65.

So, C. S., Chi, S. J., Yu, J. S., and Shelton, K.L. (1987b) The Jeonui gold-silver mine, Republic of Korea: A geochemical study: Mining Geology, V. 37, p. 313-322.

So, C. S., and Shelton, K. L. (1987a) Stable isotope and fluid inclusion studies of gold-silver-bearing hydrothermal vein deposit, Cheonan-Cheongyang-Nonsan mining district, Republic of Korea: Cheonan area: Econ. geol., v. 82, p. 987-1000.

So, C. S., and Shelton, K. L. (1987b) Fluid inclusion and stable isotope studies of gold-silver-bearing hydrothermal vein deposits, Yeoju mining district, Republic of Korea: Econ. Geol., v. 82, p. 1309-1318.

Sourirajan, S., and Kennedy, G.C. (1962) The system H_2O-Nacl at elevated temperatures and pressures: Amer. Jour. Sci., v. 260, p. 115-141.

Sugaki, A., Kim, O.J., and Kim, W.J. (1986) Gold and silver ores from the Geumwang mine in south Korea and their mineralization: Mining Geology, v. 36, p. 555-572.

Taylor, H.P. Jr. (1974) The application of oxygen and hydrogen isotope studies to problems of hydrothermal alteration and deposition: Econ. Geol., v. 69, p. 843-883.

Tsuchida, T. (1944) Ore Deposits in Korea, Kasumigaseki Book co., Tokyo, 329 p. (in Japanese).

Tsusue, A., Mizuta, T., Watanabe, M., and Min, K. G. (1981) Jurassic and Cretaceous granitic rocks in south Korea: Mining geology, v. 31, p. 1261-1280.

한반도 천안-청양-논산지역 광화대내 금-은 열수광상의 안정동위원소 및 유체포유물 연구 : 청양지역

蘇七燮, Kevin L. Shelton, 池世定, 崔尙勳

요약 : 청양지역 광화대 금-은 광상들은 화강편마암내의 단층대를 충진한 수개조의 함 금-은 열수맥상 광체로 구성된다. 광화작용의 시기는 127.1±2.8 Ma이고, 열수광화작용은 구조운동에 시기적으로 2회에 걸쳐 진행되었다. 공생광물의 유체포유물 및 안정동위원소 연구에 의하면, 초기 약 340°의 고온에서 180°에 이르는 제 I 광화시기에는 일렉트럼(42.2−66.8mole % Au), 농홍은석, 함은사면동석, 휘은석, 유비철서, 방연석, 황동석 및 섬아연석 $X_{FeS}≒0.13$)등이, $\delta^{34}S_{\Sigma S}=2-5\%$, $fs_2 <10^{-9.8}$atm., 1−8wt.% NaCl상당 염농도를 갖는 유체로부터 비등현상과 함께 침전되었다. 광화작용시의 압력은 <200−700기압이고, 광화작용의 심도는 약 1.5km였다. 열수 광화유체내 물의 수소(−90∼−130‰), 산소(−5.9∼+0.1‰)동위원소값은 광화유체의 기원이 천수임을 뜻하고, 광화유체의 비등현상과 냉각작용은 340°C이하에서 유체내 금−은 복합체 ($Au(HS)_2^-$, $AgCl_2^-$)의 파괴를 초래하여 금−은 광물의 침전을 유도하였다.

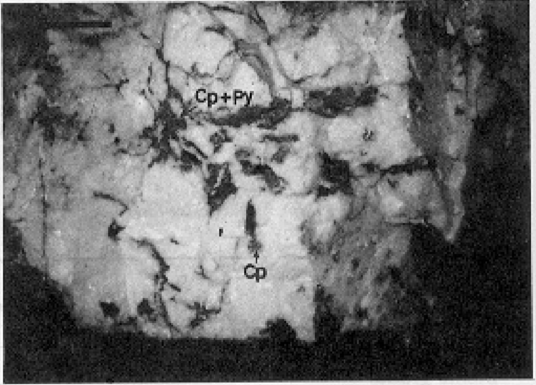
Cp+Py
Cp

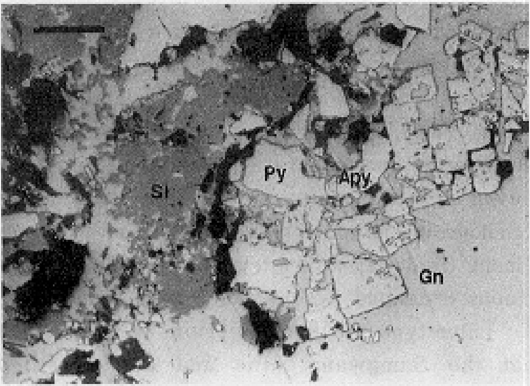

Fig. 6. Reflected light photomicrograph of stage I minerals in the Samgwang mine. Galena (Gn) replaces sphalerite (Sl) and subhedral to euhedral pyrite (Py) and arsenopyrite (Apy) along grain margins. Residual isolated sphalerite grains occur in a galena matrix. Scale bar is 0.1 ㎜.